



Contents lists available at ScienceDirect

## Computers &amp; Geosciences

journal homepage: [www.elsevier.com/locate/cageo](http://www.elsevier.com/locate/cageo)

# Efficient gravity data inversion for 3D topography of a contact surface with application to the Hellenic subduction zone

I. Prutkin<sup>a,\*</sup>, U. Casten<sup>b</sup><sup>a</sup> Delft University of Technology, Netherlands<sup>b</sup> Ruhr University of Bochum, Germany

## ARTICLE INFO

*Article history:*

Received 21 December 2006

Received in revised form

7 February 2008

Accepted 12 February 2008

*Keywords:*

Computational methods; potential fields

3D gravity data inversion

Contact surface topography

Moho boundary

Hellenic subduction zone

## ABSTRACT

We develop the theoretical foundations, numerical algorithms and computer programs to retrieve the 3D geometry of a density interface from gridded gravity data. The solution depends on constraining assumptions on permissible density values. An integral equation is solved by a new method of local corrections to find the density interface. The method is efficient and does not require trial-and-error forward modeling. We also discuss a method, based on upward and downward continuation, to isolate gravity effects from selected depth ranges. Both new methods are applied to create a model of the Moho surface for the Hellenic subduction zone. The resulting model is discussed relative to available seismic data and previous gravity analysis.

© 2008 Elsevier Ltd. All rights reserved.

## 1. Introduction

The usual approach to find 3D topography of a contact surface is forward gravity modeling. One changes an initial model in an interactive way to diminish gravity residuals. Recently this approach has been applied, for instance, to study a geological structure of the Hellenic subduction zone in Casten and Snopek (2006) by means of the package IGMAS for interactive gravity modeling, in Makris and Yegorova (2005) and in Snopek and Casten (2006). The package IGMAS (Götze and Lahmeyer, 1988) uses polyhedral bodies for 3D forward modeling, Makris and Yegorova (2005) and Snopek and Casten (2006) apply other programs (GRAVMAG and 3GRAINS, respectively), both based on rectangular prisms. The disadvantages of the forward modeling approach are particularly obvious, if we regard the package IGMAS. One changes the model of the geological section from one profile to another, but

changes in one vertical section influence the gravity field along other profiles. Each section takes into account a lot of geological and seismic a priori information, but the number of parameters, per section, is much larger than the number of profile observations, it is not reasonable from the viewpoint of stability. The problems of non-uniqueness and instability of gravity data inversion are not likely to be solved by a forward modeling approach.

A different approach is applied by Tirel et al. (2004) to obtain the Moho topography to the north of Crete; the linearized inverse problem is solved by means of the Fourier transform (Parker, 1972; Oldenburg, 1974). In our investigation we use a different procedure, we solve an integral equation for a function determining the geometry of an unknown contact surface. The kernel of this equation, evaluating the gravitational effect of a contact surface, depends in a nonlinear way on the sought function. We solve the full nonlinear 3D inverse problem by means of the method of local corrections (Prutkin, 1983, 1986) without any linearization. This method does not make use of nonlinear minimization, which reduces

\* Corresponding author. Tel.: +31 1527 87394; fax: +31 1527 82348.  
E-mail address: [I.Prutkin@tudelft.nl](mailto:I.Prutkin@tudelft.nl) (I. Prutkin).

the computer calculation time by an order of magnitude. The local corrections method takes the non-uniqueness and instability of the inverse problem into account.

Our method of inversion is of the same type, as the method of Cordell and Henderson (1968). A solution is calculated from gravity data automatically by successive approximations, without a time-consuming trial-and-error process. Like in the algorithm of Cordell and Henderson (1968), density contrast and the position of a horizontal reference plane should be specified to obtain a unique solution. We apply a different approach to form a successive approximation. Moreover, we take into account the instability of the inverse problem by means of a sort of regularization. We have mentioned above different approaches for gravity data inversion applied for the particular area of the Hellenic subduction zone. A detailed overview of the literature on the potential field inverse problem can be found in Blakely (1995).

The paper is organized as follows: we present new mathematical algorithms for isolating sources in depth and for 3D gravity data inversion, then both algorithms are applied to the Hellenic subduction zone to extract the effect of the Moho interface and find its 3D topography. We start with our mathematical theory, it is presented in the first two sections. The new algorithm is suggested as a preliminary pre-processing of gravity observations to extract the gravitational effect of the desired contact surface. The main idea of the algorithm is to eliminate sources from the Earth's surface to a prescribed depth by means of upward and downward continuation. In Section 2, the description of the algorithm is presented. The method of local corrections applied to contact surface topography recovery is developed in Section 3. Next, we start with the application of our algorithms for the Hellenic subduction zone. To avoid short wavelength intra-crustal effects, Tirel et al. (2004) band-pass filtered gravity data at 50–300 km. We apply a different approach, a model of the near-surface layer is found and its gravitational effect is subtracted from the gravity data. The short wavelength field features are related to undulations of the light sediment layer. Taking into account the results of previous modeling of sedimentary basin thickness (Makris and Yegorova, 2005; Casten and Snopek, 2006), the layer to the depth of 20 km is chosen. The model of the layer (see Section 4) demonstrates the advantages of the local corrections approach; several contact surfaces with different density contrasts have been found simultaneously. In Section 5 we extract the gravitational effect of the Moho boundary and detect its 3D topography. Section 6 contains the main conclusions of our study.

## 2. Algorithm to eliminate sources above a prescribed depth

The main purpose of the algorithm is to find the part of the observed gravity field, which is harmonic above a given depth  $h$ . We can treat this function as a gravitational effect of the half-space below the depth  $h$ . To find such a function means to eliminate all sources located in the

horizontal layer from the Earth's surface to a prescribed depth. The algorithm allows separation of the effects of shallow and deeper objects and extracts the gravity signal of sources located in horizontal layer between given depths  $h_1$  and  $h_2$ .

The algorithm is based on upward and downward continuation. There are two problems to be solved. Firstly, we continue the data from the Earth's surface upward to the height  $h$  to diminish the influence of the sources in the near-surface layer. This operation causes errors mainly in the vicinity of the boundary of the area. To reduce the errors we need a model of the regional field to subtract from the observed field prior to upward continuation. Secondly, we continue the obtained function downward to the depth  $h$ , i.e. the distance  $2h$  in downward direction. The problem of downward continuation is a linear ill-posed inverse problem, therefore we must use some regularization.

The function, which we treat as a regional field, is assumed to be harmonic in the area (in a 2D sense) and to have the same values at the boundary of the area, as the observed field:

$$\begin{cases} \Delta_2 f = \frac{\partial^2 f}{\partial x^2} + \frac{\partial^2 f}{\partial y^2} = 0 & \text{within area } S, \\ f = \Delta g & \text{on its boundary } \partial S. \end{cases} \quad (1)$$

If we subtract the values of this function, the residual field will be equal to zero at the boundary of the area, therefore no errors are introduced when we integrate the residual field while performing upward continuation along the restricted area. According to the properties of harmonic functions, this function has no extremes within the area, so we create no false anomalies. Besides, as it is known from calculus of variations (Gelfand and Fomin, 2000), a solution of problem (1) provides a minimum of the following functional:

$$J(f) = \iint_S \left( \left( \frac{\partial f}{\partial x} \right)^2 + \left( \frac{\partial f}{\partial y} \right)^2 \right) dx dy \rightarrow \min, \quad (2)$$

therefore, we obtain the smoothest possible function with given values on the boundary. All these properties allow us to regard this function as a model of the regional field.

To illustrate all steps of the algorithm, we have developed a model of the gravity field, caused by both shallow and deeper sources, as well as some objects beyond the area of investigation. The initial field and a solution of problem (1) are shown in Fig. 1.

After subtracting the suggested model of the regional field we make an upward continuation of the residual field by means of the following formula:

$$\frac{1}{2\pi} \iint \frac{h}{((x-x')^2 + (y-y')^2 + h^2)^{3/2}} U(x, y, 0) dx dy = U(x', y', h). \quad (3)$$

Formula (3) gives a solution of the Dirichlet problem: to find a harmonic function in the upper half-space with given values on the boundary (on the plane  $z = 0$ ).

At the second step we continue the obtained function downward to the depth  $h$ , i.e. the distance  $2h$  in the downward direction. To do this, we apply a formula

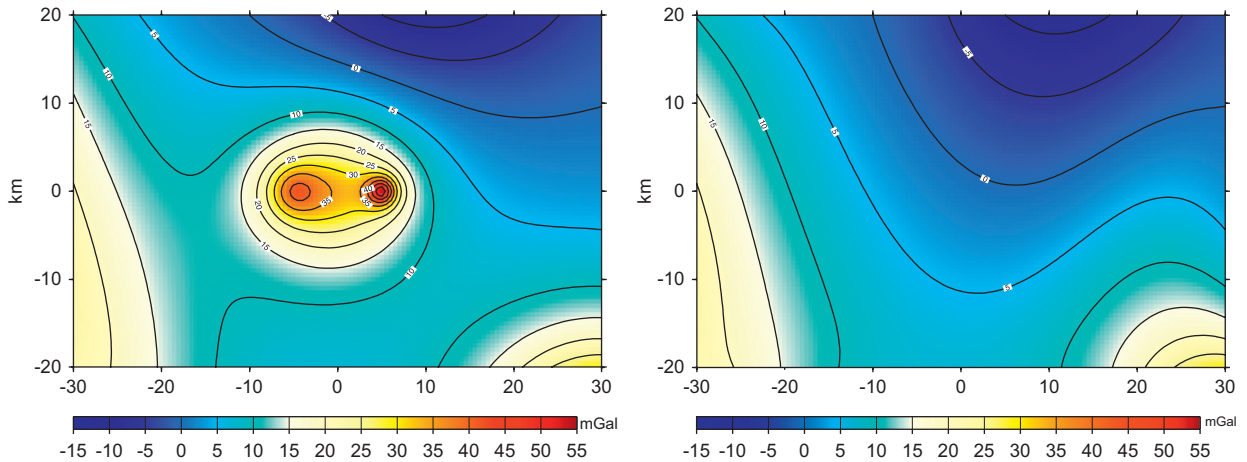


**Fig. 1.** Model of local gravity anomaly and corresponding regional field. Model of regional field (right) represents solution of problem (1), it is harmonic inside area and takes same values on boundary as given field (left).

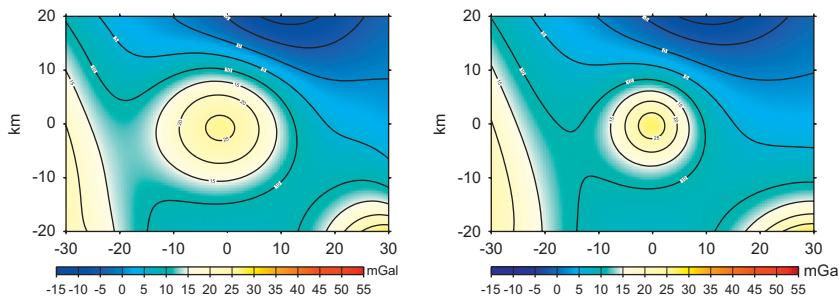


**Fig. 2.** Calculated and exact field without near-surface sources. Left panel: results of application to total field algorithm of upward and downward continuation, described in Section 2. Right panel: field of all sources but shallow ones calculated using exact formulas.

similar to (3):

$$\frac{1}{2\pi} \int \frac{h_1}{((x-x')^2 + (y-y')^2 + h_1^2)^{3/2}} U(x, y, -h) dx dy = U(x', y', h), \tag{4}$$

where  $h_1 = 2h$ . Formula (4) provides a function, which is harmonic in a half-space above the plane  $z = -h$ . This time we treat the formula as an integral equation: the right hand side is given, and we have to find the unknown function  $U(x, y, -h)$ .

Although the influence of shallow sources is diminished after the upward continuation, the rest of them are still present in the field, so we continue downward *through* the sources. It should be emphasized, that the problem of downward continuation is a linear ill-posed inverse problem, therefore we must use some regularization. Since the integral operator  $A$  in (4) is self-adjoint and positive, we apply Lavrent'ev et al.'s (1986) approach. If we write (4) in the following form:  $Au = u_h$ ,  $u$  is an unknown field on the level  $z = -h$ ,  $u_h$  is the obtained field on the height  $h$ , then Lavrent'ev's regularization gives:  $(A + \alpha I)u = u_h$ , where  $I$  is the identity operator and  $\alpha$ —a regularizing parameter. Therefore, after discretization no matrix multiplication is required.

Finally, we calculate the field on the Earth's surface  $z = 0$  using a formula similar to (3). We obtain a part of the field, which is harmonic up to the depth  $h$ , so we can treat it as an effect from the deeper sources.

The described algorithm has been applied to the model field shown in Fig. 1; an attempt is made to eliminate shallow sources and to detect the effect of the deeper objects. This time the field without near-surface sources can be found exactly. The results are presented in Fig. 2. The comparison reveals that the solution obtained by means of the suggested algorithm is slightly smoothed, but the main features have been reconstructed. It should be noted that no information beyond the area has been taken into account.

### 3. Method of local corrections

To evaluate the gravitational effect of a contact surface, we consider a model of a two-layer gravitational medium in 3D space. The model consists of two layers of a constant density  $\sigma_1$  and  $\sigma_2$ , separated by the surface  $S$ . Suppose that, in the Cartesian coordinate system, the plane  $xOy$  coincides with the Earth's surface, and the  $z$ -axis is directed downward. The upper layer is bounded above

by the horizontal plane  $z = h_-$ ,  $h_- \geq 0$ , and below by the surface  $S$ ; the lower layer is bounded above by the surface  $S$  and below by the plane  $z = h_+$ ; at  $z < h_-$  and  $z > h_+$  masses are absent. The unknown contact surface is determined by the equation  $z = z(x, y)$ . It is assumed that  $z(x, y)$  is a single-valued limited function, and that for a certain  $H$

$$\lim_{\substack{|x| \rightarrow \infty \\ |y| \rightarrow \infty}} |z(x, y) - H| = 0, \quad (5)$$

i.e., the surface  $S$  has a horizontal asymptotic plane  $z = H$ . If we subtract the effects of two Bouguer plates, we find that the field of our two-layer model accurate to a constant term is the field of masses contained between the surface  $S$  and the plane  $z = H$ , with a density  $\pm \Delta\sigma$ , where  $\Delta\sigma = \sigma_2 - \sigma_1$  is the density contrast at the contact surface. The field of such an object is evaluated by the formula

$$\Delta g(x', y', 0) = G\Delta\sigma \int_{-\infty}^{\infty} \int_{-\infty}^{\infty} \left( \frac{1}{\sqrt{(x-x')^2 + (y-y')^2 + z^2(x, y)}} - \frac{1}{\sqrt{(x-x')^2 + (y-y')^2 + H^2}} \right) dx dy, \quad (6)$$

where  $G$  is the gravitational constant. We can regard formula (6) as a nonlinear integral equation of the first kind with respect to the unknown function  $z(x, y)$ . Suppose that the field at the Earth's surface is given on a rectangular grid  $\{x_i, y_j\}$ . We divide a volume between the surface  $S$  and the plane  $z = H$  into a number of elementary prisms, for each prism the projection of its center onto the plane  $xOy$  coincides with some observation point. The mean heights of the prisms are taken as unknown parameters. Their number equals exactly to the number of observations  $N$ . We denote by  $K(x', y', x, y, z(x, y))$  the integrand in (6). This expression was referred to by [Snopek and Casten \(2006\)](#) as the gravity attraction of a linear, vertical mass. They apply it as an approximation of the exact formula for the prism gravity. It means, that while discretizing (6) by numerical integration we use one-point cubature formula for each elementary prism, which gives

$$cG\Delta\sigma \sum_i \sum_j K_{i_0 j_0}(z_{ij}) = U_{i_0 j_0}, \quad (7)$$

where  $c$  is the weight of the cubature formula,  $z_{ij} = z(x_i, y_j)$ , and

$$U_{i_0 j_0} = \Delta g(x_{i_0}, y_{j_0}, 0), \quad K_{i_0 j_0}(z_{ij}) = K(x_{i_0}, y_{j_0}, x_i, y_j, z_{ij}).$$

To increase the accuracy one could apply Gauss cubature discretization in (6), in this case each term in (7) will be substituted by several similar ones, corresponding to the same  $z_{ij}$ .

Our goal is to develop an iterative procedure for solving the system of nonlinear equations (7). Suppose that  $z_{ij}^n$  are the values of the unknown function obtained at the  $n$ -th step. For the corresponding solution of the direct problem

we introduce the notation

$$U_{i_0 j_0}^n = cG\Delta\sigma \sum_i \sum_j K_{i_0 j_0}(z_{ij}^n). \quad (8)$$

The method of local corrections is based on the fact that the variation of the field at a certain point is affected mostly by the variation of the part of the object boundary closest to this point. At each step we try to reduce the difference between the given and the approximate values of the field at a given node solely by modifying the value of the unknown function at that node. If only the value of the unknown function at one point has been changed, then the sum in (8) for the next iteration differs only in one term. Assuming that in the chosen node  $U_{ij}^{n+1} = U_{ij}$  and subtracting (8) from the similar equality corresponding to the  $(n+1)$ th step, we obtain the fundamental equation to find the next approximation ([Prutkin, 1986](#)):

$$G\Delta\sigma(K_{ij}(z_{ij}^{n+1}) - K_{ij}(z_{ij}^n)) = \alpha(U_{ij} - U_{ij}^n). \quad (9)$$

The coefficient  $\alpha$  in the right-hand side of (9) is introduced to slow down the change of the model.

It turns out that, in the case of a contact surface, Eq. (9) can be converted to a very simple form. Indeed, considering Eq. (6), we have

$$K_{ij}(z_{ij}^n) = 1/z_{ij}^n - 1/H. \quad (10)$$

Using (10), we rewrite Eq. (9) as

$$G\Delta\sigma(1/z_{ij}^{n+1} - 1/z_{ij}^n) = \alpha(U_{ij} - U_{ij}^n)$$

and finally

$$z_{ij}^{n+1} = \frac{z_{ij}^n}{1 + \alpha s z_{ij}^n (U_{ij} - U_{ij}^n)}, \quad (11)$$

where  $s = (G\Delta\sigma)^{-1}$ . According to (11), several arithmetic operations are sufficient to obtain the next successive approximation at each point of the grid. We have to store only the vector of unknowns of the same length  $N$  as the length of the observations vector. The full (nonlinear) inverse problem is solved without any linearization, and we do not need to store a matrix of the size  $N \times N$ .

For the fixed values of the density contrast  $\Delta\sigma$  and the depth to the asymptotic plane  $H$ , a solution of the inverse problem for a contact surface is unique. At the same time, different values of these parameters cause different solutions but the same gravity field. In [Prutkin \(1986\)](#), a family of contact surfaces is presented, which generate the same field, as a point source from different values of  $\Delta\sigma$  and  $H$ .

Eq. (6) is an integral equation of the first kind, this problem is ill-posed and requires regularization. Diminishing the coefficient  $\alpha$  in (11), we can prevent highly oscillating solutions, therefore this factor is similar to a regularizing parameter.

Due to the fact that our approach to inversion is local, we could take a different value of the density contrast at each grid point. One should include a function of two variables  $\Delta\sigma(x, y)$  into the integrand of Eq. (6), then use factors  $\Delta\sigma_{ij} = \Delta\sigma(x_i, y_j)$  in the left-hand side of (7) and substitute the coefficient  $s$  in (11) by  $s_{ij} = (G\Delta\sigma_{ij})^{-1}$ . The same is valid for the depth to the asymptotic plane  $H$ .

Sometimes it is reasonable to divide the whole area into sub-areas and to use different values of  $H$  and  $\Delta\sigma$  for each one. Within the method of local corrections this approach is also possible, which is demonstrated in the next section.

#### 4. Model of the layer above the depth of 20 km

We tested both algorithms described in Sections 2 and 3, on gravity data from the Hellenic subduction zone.

The Hellenic contact is an active plate boundary between Eurasian and African lithosphere. This boundary is defined by a Wadati–Benioff zone. Our area of investigation is shown in Fig. 3. Bathymetry and topography of the Hellenic plate contact, as well as the boundary of the subduction zone, is presented in Fig. 3a. As an input, the Bouguer gravity field given by Casten and Snopek (2006) is taken. Land gravity data, shipborne observations around Crete and gridded free-air anomalies deduced

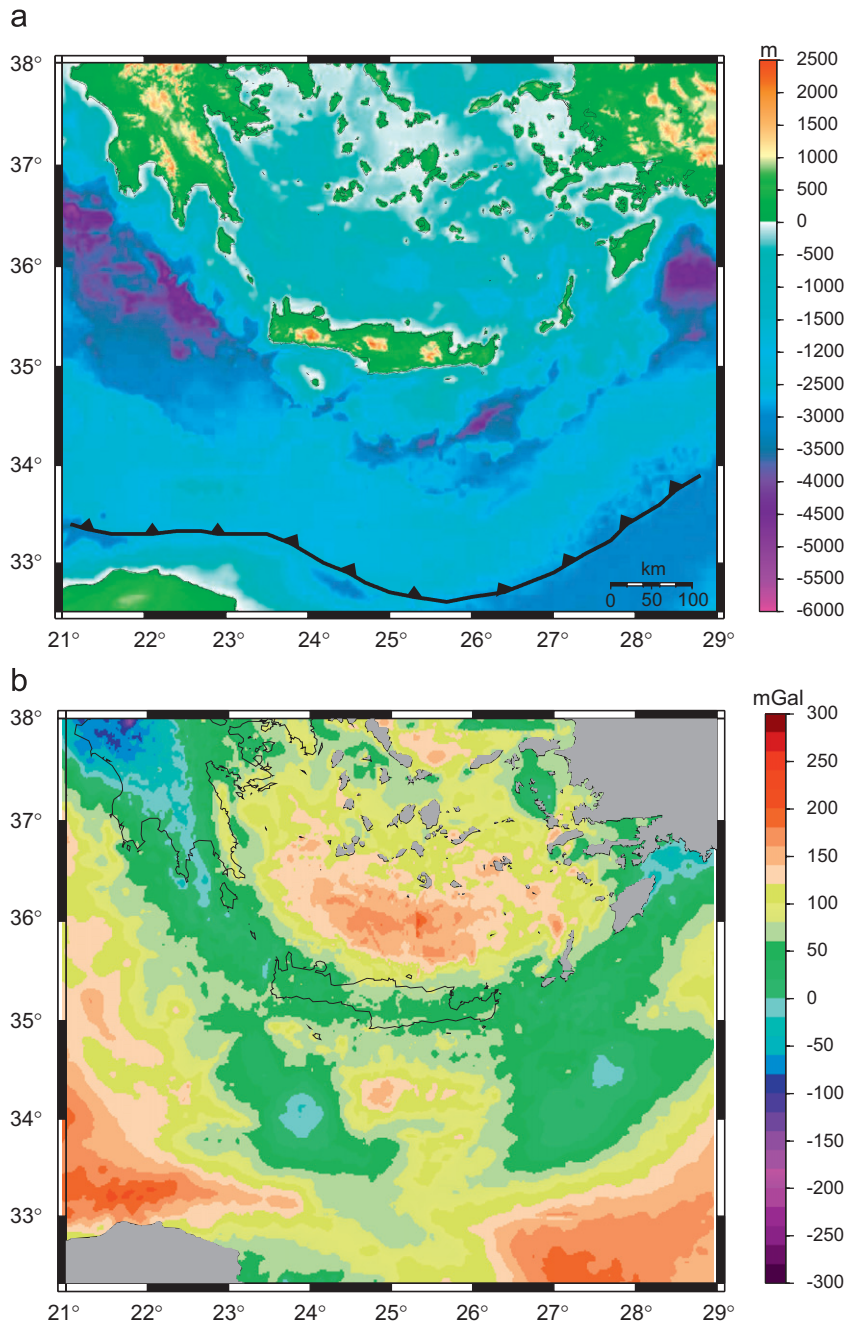


**Fig. 3.** Area of investigation. (a) Bathymetry and topography of Hellenic plate contact, boundary of subduction zone is shown. (b) Bouguer gravity field of Hellenic subduction zone. Data are corrected for mass effects of topography/bathymetry using reduction density of  $2.67 \text{ g/cm}^3$  for continental masses and of  $1.64 \text{ g/cm}^3$  for water cover in marine areas.

from satellite altimetry, were combined to produce a uniform data set. The data were corrected for mass effects of topography/bathymetry using the standard reduction density of  $2.67\text{ g/cm}^3$  for all continental masses and of  $1.64\text{ g/cm}^3$  for the water cover in marine areas. More details on how the Bouguer map was compiled can be found in Casten and Snopek (2006). The resulting Bouguer map, gridded with 1 arc min spacing, is shown in Fig. 3b.

Four regions dominate the field from north to south: (1) the gravity high (up to  $170\text{ mGal}$ ) in the Cretan Basin, (2) an arc-shaped gravity low (relative, from 0 to  $+50\text{ mGal}$ ), which connects Crete with the Peloponnesos to the west and with Anatolia to the east, (3) a variation of anomalies (from  $-10$  to  $+100\text{ mGal}$ ) outside the island, and (4) gravity highs in the south-west and in the south-east towards the African continent. Two gravity lows—one south of Crete and the other in the south-east—give rise to speculations on their origin, because they are of local character. Here, the sediments of the Mediterranean Ridge have thicknesses up to  $18\text{ km}$  (Casten and Snopek, 2006).

The main goal of our investigation is to extract the gravity signal from the Moho boundary and to find its 3D topography. From active seismic experiments (Bohnhoff et al., 2001) it is known that the continental Moho depth below central Crete is reaching  $30\text{ km}$ . To the north the Moho depth rapidly decreases to below  $20\text{ km}$  and to the south decreases gradually to  $17\text{ km}$ . About  $100\text{ km}$  off the southern coast of Crete the continental Moho is in contact with the African oceanic plate.

The area to the south of Crete is challenging to interpret: the Moho boundary in this region goes upward, according to seismic information, at the same time the gravity field is complex and includes a maximum between two local minima. We start from the model of the near-surface layer for this area.

Since we used the observations re-gridded with a spacing of  $2.5\text{ km}$ , shallow sources (above the depth of  $2.5\text{ km}$ ) have been eliminated by means of upward and downward continuation as described in Section 2. The upward and downward continuation can be regarded as a preliminary smoothing of the data. Then a density distribution in the horizontal layer between depths  $2.5$  and  $20\text{ km}$  has been found. An algorithm of gravity data inversion for a square density distribution can be derived from the main equation (9). In this case the inverse problem becomes linear, the same is true of the formula to obtain the next approximation. It is known that one can find a density distribution in a near-surface layer (or even in a simple layer), which is responsible for the total observed gravity. To prevent this, we have developed the following approach: a density variation is limited according to a priori information, it is allowed to vary from  $2.3$  to  $2.85\text{ g/cm}^3$  (see Makris and Yegorova, 2005; Casten and Snopek, 2006). In this way, the part of the total field caused by shallow sources can be extracted.

At the next step we transform the horizontal layer with density distribution into a piecewise homogeneous medium with two contact surfaces. It is observed that the mean density value is equal to  $2.6\text{ g/cm}^3$ . If we subtract the mean density value, the area will be divided into sub-areas with negative and positive density variations

relative to the mean value. We introduce two generalized types of geological section: in the sub-areas, where the density is less than its average value, we suppose the presence of the material with density  $2.3\text{ g/cm}^3$  from the depth of  $2.5\text{ km}$  up to a contact surface and with density  $2.6\text{ g/cm}^3$  below the contact surface to the depth of  $20\text{ km}$ ; in the sub-areas with positive density variation the material is assumed to have density  $2.6\text{ g/cm}^3$  from  $2.5\text{ km}$  up to a contact surface and  $2.85\text{ g/cm}^3$  from the contact surface to the depth of  $20\text{ km}$ . All average density values are identical to those published by Makris and Yegorova (2005).

The initial position of the unknown contact surfaces were obtained in such a way that the mass of each elementary prism coincides with the mass of the homogeneous prism with density from the estimated density distribution. Then the solution has been further improved by means of the method of local corrections presented in Section 3. The process could be described in the following way: we start from the homogeneous layer with average density of  $2.6\text{ g/cm}^3$ , then in “negative” sub-areas the boundary of light material moves downward from the depth of  $2.5\text{ km}$ , in “positive” sub-areas the boundary of more dense material moves upward from the depth of  $20\text{ km}$ . It should be noted that in the framework of our approach it is possible to take different values of the density contrast  $\Delta\sigma$  and the depth to the asymptotic plane  $H$  for different sub-areas.

The obtained model of the area is shown in Fig. 4. We should repeat that our goal at this step is to remove gravity anomalies caused by near-surface density variations to the south of Crete. Only this smaller area is shown, which represents a part of the entire area of investigation. To calculate the depth to the contact surface, one has to subtract negative values from  $2.5\text{ km}$  and positive values from  $20\text{ km}$ . The model includes two depressions of the light sediment layer and an uplift of the crystalline basement between them. This model is quite similar to the results of Makris and Yegorova (2005) (see Fig. 10, where a WE-oriented section for the same area is presented). As distinct from Makris and Yegorova (2005), our results have been obtained automatically without any forward modeling.

## 5. Gravitational effect and 3D topography of the Moho boundary

The gravitational effect of the near-surface layer model obtained in the previous section has been subtracted from the observed field. It is known that this procedure generates high-frequency disturbances in the residual field. We could treat these disturbances as artificial shallow sources. Therefore, it seems to be quite suitable to apply the algorithm of upward and downward continuation from Section 2 to eliminate the sources. The residual field after this processing is shown in Fig. 5. Now the gravity field has a minimum at Crete and then increases to the south, just in agreement with the behavior of the Moho boundary according to seismic data.

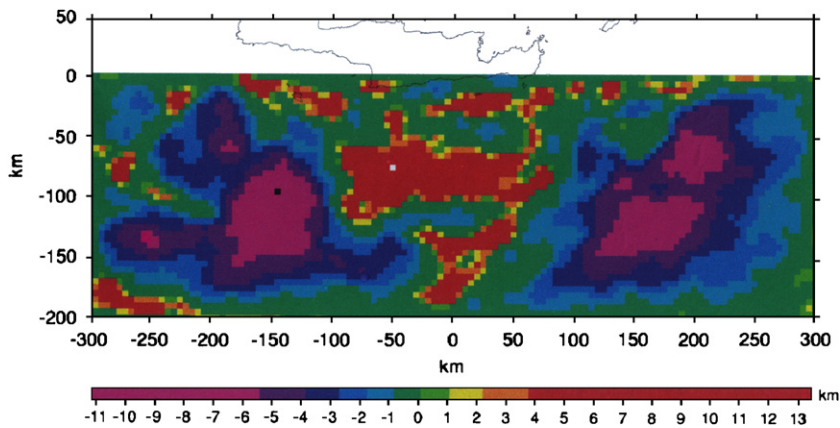


**Fig. 4.** Model of near-surface layer. “Negative” sub-areas represent depressions of light sediment layer with density  $2.3 \text{ g/cm}^3$  from depth of 2.5 km, to obtain real depth one has to subtract negative value from 2.5 km. In “positive” sub-area there is uplift of crystalline basement with density  $2.85 \text{ g/cm}^3$  from depth of 20 km, to obtain real depth one has to subtract positive value from 20 km.

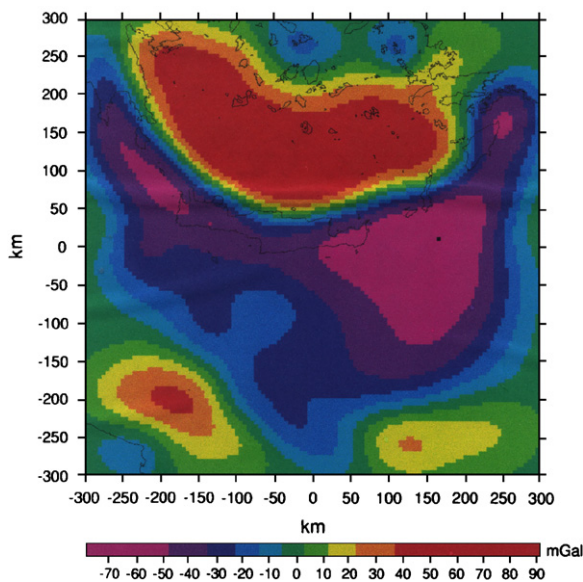


**Fig. 5.** Field without shallow sources. Gravitational effect of near-surface layer model is subtracted from initial data, short wavelength features are eliminated by means of algorithm from Section 2.

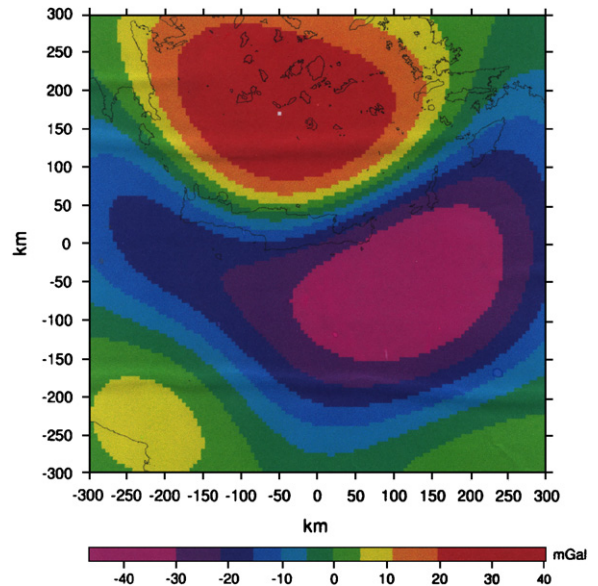


**Fig. 6.** Field of deeper sources. Sources up to depth of 100 km are removed using algorithm of upward and downward continuation, described in Section 2.

We try to find the depth of the continental Moho (the contact surface between lower continental crust and European lithospheric mantle). The only problem we have now is that the residual field in Fig. 5 looks extremely asymmetric in WE direction. It does not correspond to seismic information (Makris and Yegorova, 2005) and results of the previous modeling (Makris and Yegorova, 2005; Snopek and Casten, 2006) for the Moho boundary. These considerations have led us to the conclusion that we have not extracted yet the gravitational signal of the Moho boundary in the proper way. It is supposed that the residual field in Fig. 5 still represents a sum of two effects: from the Moho boundary itself and from deeper sources.

To separate the effects we apply again the algorithm described in Section 2. This time the part of the residual

field has been found, which is harmonic above the depth of 100 km. The gravitational signal from the half-space below 100 km is presented in Fig. 6. It consists of the positive anomaly with the shape close to the Aegean Microplate and the negative anomaly in the area of the Mediterranean Ridge. The possible source of this field could be an uplift of light asthenosphere material in the area of subduction. After subtracting the effect of deeper sources (Fig. 6) from the residual field (Fig. 5) we obtain ultimately the field, which is regarded as the gravitational signal from the Moho boundary. This field is shown in Fig. 7.

Using the obtained field as given data, we solve the inverse problem for a 3D topography of the Moho boundary. The method of local corrections is applied,

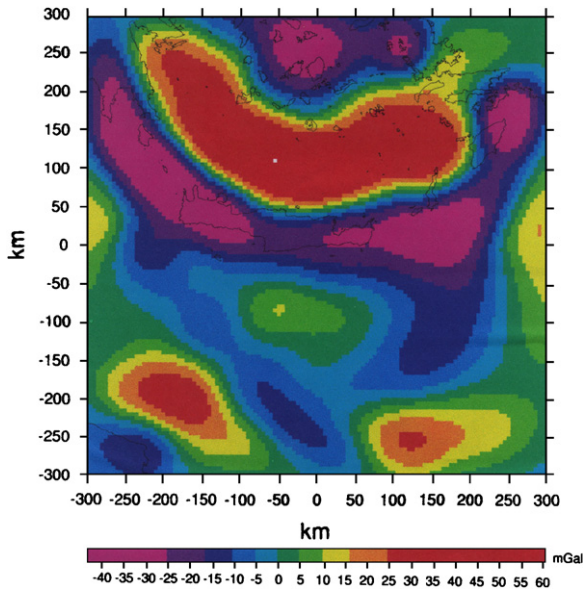


Fig. 7. Effect of Moho boundary. To obtain field, gravity effects from near-surface layer up to depth of 20 km and from half-space below 100 km are subtracted from initial data.

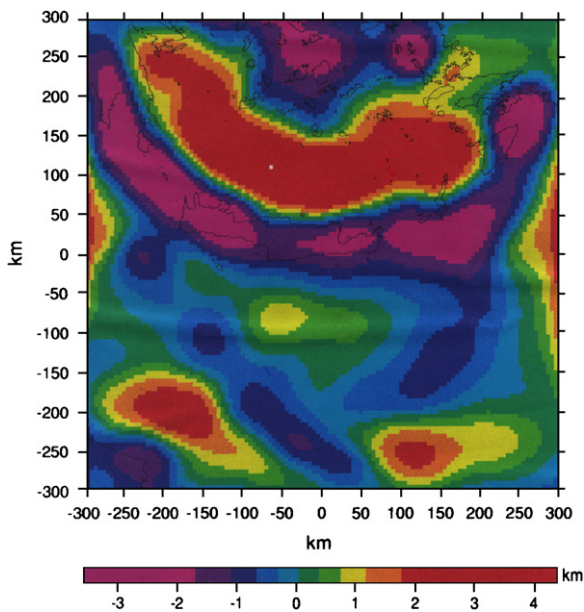


Fig. 8. Topography of Moho boundary. Geometry of contact surface is obtained by means of method of local corrections, described in Section 3. Undulations from depth of 20 km are shown, to obtain real depth one has to subtract both positive and negative values from 20 km.

which is described in Section 3. The density distribution for the upper layer has been discussed beforehand. The lower layer is assumed to be homogeneous with density of  $3.3 \text{ g/cm}^3$  (Snopek and Casten, 2006). Since the upper layer is non-homogeneous, a density contrast has different values at different grid points, which is quite admissible in the framework of the method of local corrections (see

Section 3). We take the value  $H = 20 \text{ km}$  as a depth to the asymptotic plane. The obtained 3D topography of the Moho boundary is shown in Fig. 8. The difference between the depth to the asymptotic plane  $H = 20 \text{ km}$  and the depth to the Moho boundary is displayed (the value  $+5 \text{ km}$  means the depth  $15 \text{ km}$ , the value  $-5$ ,  $25 \text{ km}$ , respectively). The depth to the obtained Moho boundary has a minimum to the north of Crete, a maximum below Crete, then the depth decreases gradually to the south. The main features of the obtained topography are quite in agreement with seismic information and results of previous gravity modeling. Moreover, as distinct from Makris and Yegorova (2005) and Snopek and Casten (2006), the gravitational maximum at the center of Crete is reproduced.

It should be noted that several assumptions are made to obtain such a solution. While calculating the model of the near-surface layer, we have certain limiting restrictions on density variation according to a priori information. We assume also that all singularities related to the Moho boundary are located above the depth of 100 km, which allows us to eliminate deeper sources. These assumptions make it possible to isolate the contribution of the Moho surface from the total field. Prior to solving the inverse problem by means of the method of local corrections, the density contrast and the depth to the asymptotic plane are specified according to seismic data.

## 6. Summary and conclusions

Two new algorithms have been suggested to extract the signal from a contact surface and to find its 3D geometry. Both algorithms are applied to gravity data for the Hellenic subduction zone to recover the Moho boundary topography. The following conclusions are drawn:

- (1) A new algorithm has been suggested to eliminate the sources from the Earth's surface to a prescribed depth  $h$ , based on upward and downward continuation. This algorithm can separate the effects of shallow and deeper objects. The solution of the 2D Dirichlet problem can be used as a model of the regional field. Subtracting the regional field from the observations prior to upward continuation allows integration of gravity data in the restricted area, while ignoring any information beyond the area of investigation. Downward continuation provides the part of the field, which is harmonic above the depth  $h$ . The properties of the integral operator give an opportunity to implement Lavrent'ev's regularization and to get rid of matrix multiplication.
- (2) The method of local corrections is developed to recover 3D topography of a contact surface. The method offers a simple and effective procedure for solving the nonlinear inverse problem without any linearization. This method does not make use of nonlinear minimization, which reduces the computer calculation time by an order of magnitude. We solve an integral equation for the function determining a topography. Density contrast

and the depth to the asymptotic plane must be specified to obtain a unique solution. We take into account instability of the inverse problem by means of a sort of regularization.

- (3) Both algorithms were applied to the Hellenic subduction zone. The algorithm of upward and downward continuation has eliminated near-surface and deeper sources. A density distribution for the layer to the depth of 20 km has been found, which is transformed into two contact surfaces with different density contrasts found simultaneously by means of the method of local corrections. This method is applied also after isolating the gravitational effect of the Moho boundary to recover its 3D topography. Several preliminary assumptions are made: restricted amplitude of density variation in the near-surface layer, depth to singularities related to the Moho boundary, density contrast and the depth to the asymptotic plane for the Moho surface. But all these assumptions are made prior to solving the inverse problem. The inversion itself is made automatically without interactive forward modeling which dramatically diminishes the time expenditure.

### Acknowledgments

All interpretation of gravity data for the Hellenic subduction zone has been carried out during a short term stay of I. Prutkin at the Ruhr University of Bochum (Germany) supported by German Research Foundation (DFG) within the frame of the Collaborative Research Centre 526. This support is gratefully acknowledged.

### References

- Blakely, R.J., 1995. *Potential Theory in Gravity and Magnetic Applications*. Cambridge University Press, Cambridge, 441pp.
- Bohnhoff, M., Makris, J., Papanikolaou, D., Stavrakakis, G., 2001. Crustal investigation of the Hellenic subduction zone using wide aperture seismic data. *Tectonophysics* 343, 239–262.
- Casten, U., Snopek, K., 2006. Gravity modelling of the Hellenic subduction zone—a regional study. *Tectonophysics* 417, 183–200.
- Cordell, L., Henderson, R.G., 1968. Iterative three-dimensional solution of gravity anomaly data using a digital computer. *Geophysics* 33, 596–601.
- Gelfand, I.M., Fomin, S.V., 2000. *Calculus of Variations*. Dover Publications, New York, 240pp.
- Götze, H.-J., Lahmeyer, B., 1988. Application of three-dimensional interactive modelling in gravity and magnetics. *Geophysics* 53, 1096–1108.
- Lavrent'ev, M.M., Romanov, V.G., Shishatskii, S.P., 1986. *Ill-Posed Problems of Mathematical Physics and Analysis*. Translations of Mathematical Monographs, vol. 64, American Mathematical Society, Providence, 290pp.
- Makris, J., Yegorova, T., 2005. A 3-D density–velocity model between the Cretan Sea and Libya. *Tectonophysics* 417, 201–220.
- Oldenburg, D., 1974. The inversion and interpretation of gravity anomalies. *Geophysics* 39, 526–536.
- Parker, R., 1972. The rapid calculation of potential anomalies. *Geophysical Journal of the Royal Astronomical Society* 31, 447–455.
- Prutkin, I.L., 1983. Approximate solution of three-dimensional gravimetric and magnetometric inverse problems by the method of local corrections. *Izvestiya USSR Academy Sciences, Physics of the Solid Earth* 19 (1), 38–41.
- Prutkin, I.L., 1986. The solution of three-dimensional inverse gravimetric problem in the class of contact surfaces by the method of local corrections. *Izvestiya USSR Academy of Sciences, Physics of the Solid Earth* 22 (1), 49–55.
- Snopek, K., Casten, U., 2006. 3GRAINS: 3D gravity interpretation software and its application to density modeling of the Hellenic subduction zone. *Computers & Geosciences* 32 (5), 592–603.
- Tirel, C., Gueydan, F., Tiberi, C., Brun, J.-P., 2004. Aegean crustal thickness inferred from gravity inversion. Geodynamical implications. *Earth and Planetary Science Letters* 228, 267–280.